

T.Y. Jeon  
H.-J. Kim  
S.-K. Chung  
H.-J. Dhong  
H.Y. Kim  
Y.J. Yim  
S.T. Kim  
P. Jeon  
K.H. Kim

# Sinonasal Inverted Papilloma: Value of Convoluted Cerebriform Pattern on MR Imaging

**BACKGROUND AND PURPOSE:** A convoluted cerebriform pattern (CCP) has been reported as a valuable MR imaging feature of inverted papilloma (IP). The purpose of this study was to validate the usefulness of CCP for distinguishing IP from various malignant sinonasal tumors in a relatively large number of patients.

**MATERIALS AND METHODS:** We retrospectively reviewed MR images of 30 patients with IP and 128 patients with various malignant sinonasal tumors proved on histologic examination and compared the prevalence of a CCP between the 2 groups. In 8 patients with IP concomitant with squamous cell carcinoma, we also tried to find the MR features to help suggest coexistent malignancy.

**RESULTS:** A CCP was demonstrated in all 30 (100%) of the IPs and 17 (13%) of the 128 malignant sinonasal tumors on MR imaging. There was a significant statistical difference in the prevalence of a CCP between IP and malignant sinonasal tumors with the overall sensitivity, specificity, positive predictive value, negative predictive value, and accuracy 100%, 87%, 64%, 100%, and 89%, respectively. Of 8 IPs concomitant with squamous cell carcinoma, a focal loss of a CCP was demonstrated in 4 tumors, 3 of which also showed aggressive bone destruction with extrasinonasal extension on MR images.

**CONCLUSION:** Although a CCP is a reliable MR imaging feature of sinonasal IPs, it can also be seen in various malignant sinonasal tumors. A focal loss of a CCP might be a clue to the diagnosis of IPs concomitant with malignancy.

Inverted papilloma (IP) is an uncommon benign epithelial tumor of the sinonasal tract, accounting for 0.5% to 4.0% of primary nasal tumors.<sup>1,2</sup> Although benign, it has a known propensity for a high rate of recurrence, local aggressiveness, multicentricity, and association with synchronous or metachronous squamous cell carcinoma (SCC).<sup>3-12</sup> Although CT and MR imaging are useful for preoperative assessment of sinonasal IP, differentiation of IP from other malignant sinonasal tumors is often difficult because of a significant overlap of the imaging features.<sup>13-19</sup>

Barnes et al<sup>20</sup> described a distinctive gross mucosal morphology of IP, a so-called convoluted cerebriform pattern (CCP), which can be reflected on MR imaging by the characteristic alternating hypointense and hyperintense bands on T2-weighted and contrast-enhanced T1-weighted images, as reported by Ojiri et al<sup>17</sup> and supported by Maroldi et al<sup>19</sup> years later. It would be useful for planning therapeutic strategies if the CCP on MR imaging can suggest the preoperative diagnosis of IP, because more aggressive surgical approaches would be needed for IPs concomitant with SCC and other malignant sinonasal tumors. However, one previous study reported by Yousem et al<sup>13</sup> failed to find this sign as a specific MR imaging finding to diagnose IP. The purpose of this study was to evaluate the diagnostic accuracy of a CCP depicted on MR imaging for distinguishing IP from other malignant sinonasal tumors in a relatively large number of patients.

## Materials and Methods

### Patients

From 1995 to 2006, search of the electronic data base of our institution, approved by our institutional review board, revealed a total of 132 patients with sinonasal IP proved on pathologic examination. Of these 132 patients, MR examination was performed in 33 patients. Three patients were excluded from the study because of suboptimal image quality ( $n = 1$ ) and too small lesion to be seen on MR images ( $n = 2$ ), resulting in 30 patients who formed the subjects of this study. There were 24 men and 6 women, ranging in age from 40 to 85 years, with a mean age of 63 years. All of the patients underwent surgical excision of the tumor, which disclosed that the tumor primarily involved the nasal cavity ( $n = 22$ ), maxillary sinus ( $n = 13$ ), ethmoid sinus ( $n = 3$ ), and sphenoid sinus ( $n = 2$ ). Bilaterality was found in 4 patients. Only 1 patient had the tumor confined to the nasal cavity, and in the other 29 patients, the tumor involved the adjacent sinonasal cavity from its original site. The mean tumor size was 4.8 cm in greatest diameter, ranging from 2.1 cm to 7.3 cm. Eight (8 of 30 [27%]) patients had coexistent SCC on histologic examination.

To validate the role of CCP for distinguishing IP from other sinonasal tumors, we selected MR images of 128 adult patients with 14 different types of malignant sinonasal tumors through a search of the electronic data base of our institution during the same period by using the keywords "malignant tumor of the nose and paranasal sinuses." All of the patients except for those with lymphoma and rhabdomyosarcoma underwent curative or palliative surgical resection. These 128 patients consisted of 107 men and 23 women with their age range from 20 to 84 years (mean, 58 years). Their pathologic subtypes included SCC ( $n = 49$ ), lymphoma ( $n = 39$ ), adenoid cystic carcinoma ( $n = 10$ ), malignant melanoma ( $n = 8$ ), adenocarcinoma ( $n = 5$ ), rhabdomyosarcoma ( $n = 4$ ), esthesioneuroblastoma ( $n = 3$ ), plasmacytoma ( $n = 3$ ), primitive neuroectodermal tumor ( $n = 2$ ), and 1 case each of ameloblastic carcinoma, chordoma, mucoepidermoid carcinoma, undifferentiated carcinoma, and nonkeratinizing carcinoma.

Received February 9, 2008; accepted after revision March 17.

From the Departments of Radiology (T.Y.J., H.-J.K., Y.J.Y., S.T.K., P.J., K.H.K.) and Otorhinolaryngology-Head and Neck Surgery (S.-K.C., H.-J.D., H.Y.K.), Samsung Medical Center, Sungkyunkwan University School of Medicine, Seoul, Korea.

Please address correspondence to Hyung-Jin Kim, Department of Radiology, Samsung Medical Center, Sungkyunkwan University School of Medicine, 50 Ilwon-Dong, Kangnam-Ku, Seoul 135-710, Korea; E-mail: hyungkim@skku.edu

DOI 10.3174/ajnr.A1128

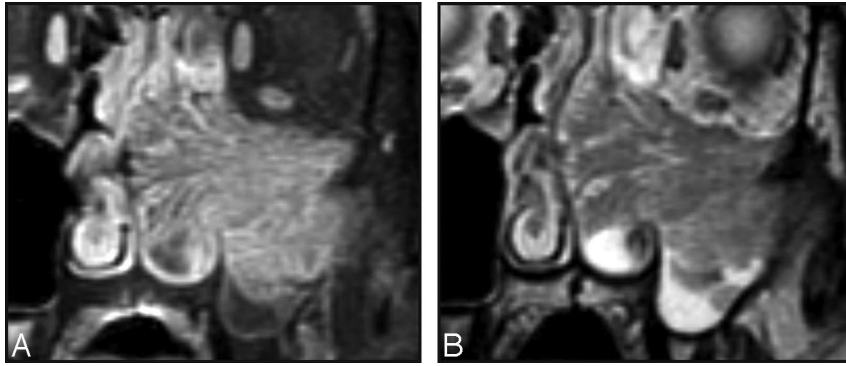


**Fig 1.** Characteristic MR imaging appearance of a CCP in IP. Coronal T2-weighted (A) and contrast-enhanced fat-suppressed T1-weighted (B) MR images show alternating hypointense and hyperintense striations throughout the tumor involving the left maxillary sinus and nasal cavity.

### MR Imaging

All of the MR examinations were performed on a 1.5T (Signa Advantage Horizon; GE Healthcare, Milwaukee, Wis) or 3T (Intera Achieva; Philips, Best, the Netherlands) scanner. In all of the patients, precontrast T1-weighted spin-echo images (TR/TE/NEX, 400–560 ms/10–14 ms/2) and T2-weighted fast spin-echo images (TR/TE/NEX, 2500–4500 ms/80–110 ms/1) with or without fat saturation were obtained, followed by contrast-enhanced T1-weighted spin-echo images with fat saturation after the intravenous injection of 0.1 mmol/kg of gadopentetate dimeglumine. Images were obtained in at least 2 planes with 3- to 4-mm section thickness, 0- to 1-mm intersection gap, 256 × 192 matrix, and 22-cm FOV.

### Image Analysis

All of the MR images were retrospectively reviewed by a dedicated head and neck neuroradiologist and a general neuroradiologist in conference, who have been practicing in the field for 18 years and 11 years, respectively. Both observers were blinded to the final histopathology. We determined the presence or absence of a CCP on MR imaging in 30 patients with IP and 128 patients with various malignant sinonasal tumors. We defined a CCP as a mix of linear or curvilinear hyperintense and hypointense striations partially or diffusely seen in the solid components of the tumor on T2-weighted or contrast-enhanced T1-weighted MR images (Fig 1). In 30 patients with IP, we compared the detection rate of CCP between T2-weighted and contrast-enhanced T1-weighted images. The image quality demonstrating CCP between the 2 sequences was also compared by subjective assessment. Statistical differences of CCP between IP and malignant sinonasal tumors were analyzed by Fisher exact test, and a *P* value of less than .05 was considered statistically significant. We also determined the sensitivity, specificity, positive predictive value, negative predictive value, and accuracy of a CCP for the diagnostic indicator of IP. In 8 patients with concomitant IP and SCC, we also tried to find the associated, if any, valuable MR imaging features to help suggest coexistent malignancy.

### Results

The prevalences of a CCP depicted on MR imaging in IP and malignant sinonasal tumors with various histology are summarized in the Table. There was a significant statistical difference in the prevalence of a CCP between IP and other malignant sinonasal tumors (*P* < .0001).

A CCP was demonstrated on MR imaging in all 30 of the IPs either diffusely (*n* = 26) or partially (*n* = 4). Contrast-enhanced T1-weighted images were better than T2-weighted images to visualize a CCP in these patients, not only in the detection but also in the image quality (Table). Contrast-en-

**Comparison of visualization of a CCP on MR imaging between inverted papilloma and various malignant sinonasal tumors**

Tumor	No. of Total Subjects	No. of Subjects Showing CCP on MR Imaging			
		Diffuse	Partial	T2WI	CE-T1WI
Inverted papilloma	30	26	4	28	30
Without SCC	22	22	0	20	22
With SCC	8	4	4	8	8
Malignant tumors	128	6	11	13	17
SCC	49	2	6	6	8
Lymphoma	39	0	0	0	0
Adenoid cystic carcinoma	10	1	1	1	2
Malignant melanoma	8	0	1	0	1
Adenocarcinoma	5	1	0	1	1
Rhabdomyosarcoma	4	0	0	0	0
Esthesioneuroblastoma	3	0	2	2	2
Plasmacytoma	3	0	0	0	0
Primitive neuroectodermal tumor	2	1	0	1	1
Ameloblastic carcinoma	1	0	0	0	0
Chordoma	1	0	0	0	0
Mucoepidermoid carcinoma	1	1	0	1	1
Undifferentiated carcinoma	1	0	1	1	1
Non-keratinizing carcinoma	1	0	0	0	0

**Note:**—CCP indicates convoluted cerebriform pattern; T2WI, T2-weighted image; CE-T1WI, contrast-enhanced T1-weighted image; SCC, squamous cell carcinoma.

hanced T1-weighted images detected a CCP in all (100%) of the IPs, whereas T2-weighted images detected a CCP in 28 (93%). Furthermore, in 28 IPs where a CCP was seen on both T2-weighted and contrast-enhanced T1-weighted images, the quality of the latter was as good as (*n* = 13) or better than (*n* = 15) that of the former. In all 22 of the IPs without associated SCC, CCP was shown diffusely throughout the tumor. There was no case showing aggressive bone destruction, extrasinonasal extension, or intratumoral necrosis in these tumors. In contrast, in 8 IPs concomitant with SCC, the areas of a focal loss of a CCP were demonstrated in 4 (50%), 3 of which also showed aggressive bone destruction with extrasinonasal extension on MR images (Fig 2A). Intratumoral necrosis was also noted in 2 of these 3 cases. The remaining 4 tumors showed CCP throughout the lesion, identical to the tumors without SCC (Fig 2B). The histology in these 4 tumors revealed multiple foci of microscopic carcinoma within the tumor.

Of the 128 malignant sinonasal tumors with various histology, 17 tumors (13%) demonstrated a CCP on MR imaging



**Fig 2.** MR images of the IP concomitant with SCC in 2 different patients. *A*, Coronal contrast-enhanced, fat-suppressed, T1-weighted image shows a large irregular mass in the right nasal cavity and maxillary sinus. Although the nasal mass displays the characteristic CCP, it is lost in most of the mass of the maxillary sinus. Note the bone destruction at the superior and lateral walls of the maxillary sinus with associated orbital invasion (*arrows*). *B*, Axial contrast-enhanced, fat-suppressed, T1-weighted image shows an expansile mass in the left nasal cavity, which displays a diffuse CCP throughout the lesion, indistinguishable from the IP without associated carcinoma. The histology revealed multiple foci of microscopic carcinoma scattered within the tumor.

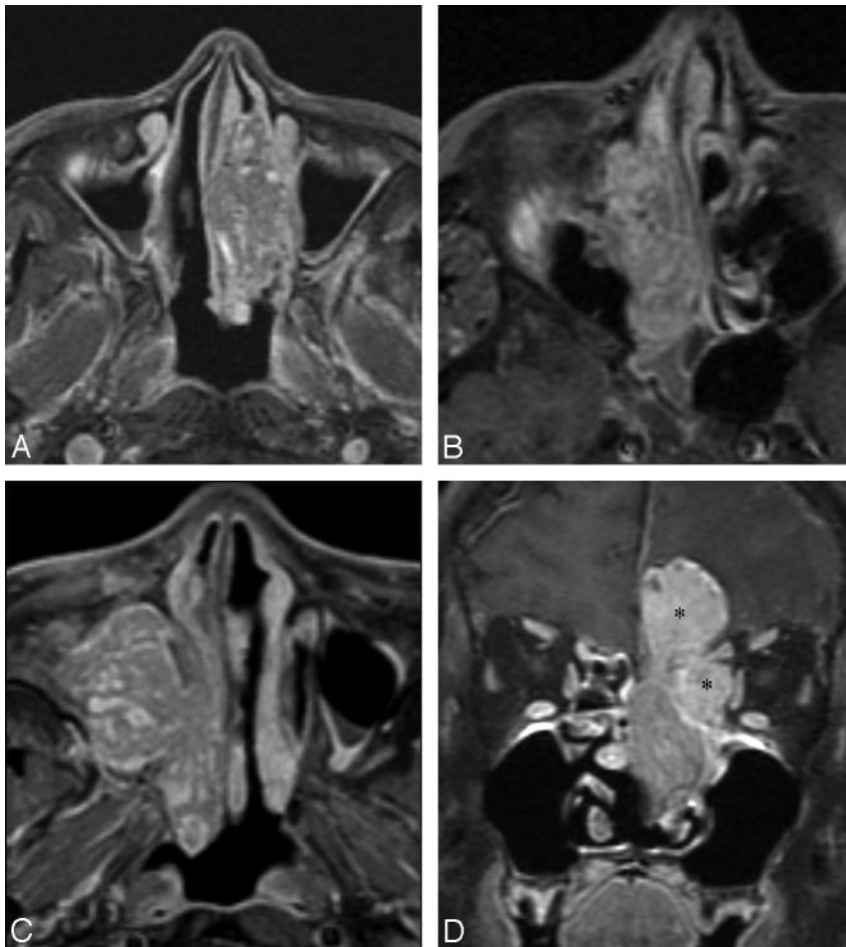


**Fig 3.** Contrast-enhanced fat-suppressed MR images of 4 different malignant sinonasal tumors displaying a CCP either diffusely (*A–C*) or partially (*D*). *A*, SCC. *B*, Primitive neuroectodermal tumor. *C*, Mucoepidermoid carcinoma. *D*, Esthesioneuroblastoma. In the case of esthesioneuroblastoma, the MR image shows a large mass in the left nasal cavity, extending to the orbit and cranial cavity. Note that, whereas the nasal component of the mass displays a typical appearance of CCP, it is not seen in the rather homogeneously enhancing orbital and intracranial components (*asterisks* in *D*).

either diffusely ( $n = 6$ ; Fig 3A–C) or partially ( $n = 11$ ; Fig 3D) and included 8 of 49 SCCs (Fig 3A), 2 of 10 adenoid cystic carcinomas, 2 of 3 esthesioneuroblastomas (Fig 3D), 1 of 8 malignant melanomas, 1 of 5 adenocarcinomas, 1 of 2 primitive neuroectodermal tumors (Fig 3B), 1 of 1 mucoepidermoid carcinoma (Fig 3C), and 1 of 1 undifferentiated carcinoma. Bone destruction was noted in 1 of 6 tumors with a diffuse CCP and 9 of 11 tumors with a partial CCP. Overall, the sensitivity, specificity, positive predictive value, negative predictive value, and accuracy of CCP for the diagnosis of IP were 100% (95% confidence interval [CI], 90%–100%), 87%

(95% CI, 80%–92%), 64% (95% CI, 50%–76%), 100% (95% CI, 97%–100%), and 89% (95% CI, 84%–93%), respectively.

### Discussion

According to the World Health Organization, IP is defined as a benign epithelial tumor composed of well-differentiated columnar or ciliated respiratory epithelium having variable squamous differentiation.<sup>21</sup> Embryologically, the ectodermally derived epithelium of IP originating from the Schneiderian mucosa of the nasal cavity is distinct from the endodermally derived mucosa of the upper respiratory tract.<sup>12</sup>

Complete surgical resection is crucial to reduce the recurrence rates, which have ranged from 15% to 78%.<sup>6-8</sup> Preoperative evaluation by using cross-sectional imaging, such as CT and MR imaging, is essential for the selection of surgical options by correctly identifying the location and extent of the tumor, and postoperative follow-up examinations at regular intervals are also highly recommended for the early detection of the recurrent disease.<sup>11-18,22-24</sup> However, differentiation of IP from other malignant sinonasal tumors by analyzing the internal characteristics on radiologic imaging is often difficult, because there is a significant overlap between those diseases.<sup>15,16,19</sup>

IP is seen pathologically as a vascular mass with prominent mucous cyst inclusions interspersed throughout the epithelium and a high intracellular glycogen content.<sup>3,20</sup> The name is a descriptive term of the histology that shows inversion of the surface epithelium into the underlying stroma rather than exophytic proliferation.<sup>5,15</sup> On physical examination, IP presents as a polypoid growth covered by a convoluted cerebriform mucosa, called a CCP, as described by Barnes et al.<sup>20</sup> This gross morphology, created by the juxtaposed epithelial and stromal layers, results in a peculiar pattern on MR imaging, manifesting as the alternating hypointense and hyperintense bands, which has been described under the various terms.<sup>13,17,19</sup> Yousem et al<sup>13</sup> used the term “septate striated appearance” and noticed it in 5 (50%) of 10 patients with IP on T2-weighted images. However, the researchers did not impart much importance to it because it was also seen in 2 of 8 other sinonasal malignancies. Ojiri et al<sup>17</sup> used the term “CCP” and found it in 8 (80%) of 10 patients with IP on T2-weighted and contrast-enhanced T1-weight images. The radiologic-pathologic correlation revealed that the highly cellular metaplastic epithelium was seen as the thinner hypointense striations on T2-weighted images and less enhancing striations on contrast-enhanced T1-weighted images, whereas the less cellular edematous stroma was seen as the thicker hyperintense striations on T2-weighted images and well-enhancing striations on contrast-enhanced T1-weighted images.<sup>17</sup> However, they did not evaluate the prevalence of this MR imaging feature in other malignant sinonasal tumors. In their study with 23 patients with IP, Maroldi et al<sup>19</sup> coined the term “columnar pattern” and observed it in 16 patients (69.5%) on T2-weighted images and 23 patients (100%) on contrast-enhanced T1-weighted images. In their study, this columnar pattern was identified in only 1 (4.3%) of 23 other malignant sinonasal tumors on both T2-weighted and contrast-enhanced T1-weighted images.

Our study showed a significant statistical difference in the prevalence of a CCP between IP (30 of 30 [100%]) and other malignant sinonasal tumors (17 of 128 [13%]) with the overall sensitivity, specificity, positive predictive value, negative predictive value, and accuracy of CCP for the diagnosis of IP at 100%, 87%, 64%, 100%, and 89%, respectively. Our study also showed that the contrast-enhanced T1-weighted images were superior to the T2-weighted images in the detection of a CCP (30 of 30 [100%] versus 28 of 30 [93%]), as reported by Maroldi et al.<sup>19</sup> Furthermore, the quality of contrast-enhanced T1-weighted images was at least as good as that of T2-weighted images in all of the patients with IP. The superiority of the contrast-enhanced T1-weighted images might be attributed to the vascular nature of the tumor, which would become more conspicuous after the injection of contrast material. In our

study, however, a considerable number of false-positive cases (17 of 128 [13%]), which was lower than those (2 of 8 [25%]) of Yousem et al<sup>13</sup> but higher than those (1 of 30 [4.3%]) of Maroldi et al,<sup>19</sup> resulted in the overall diagnostic accuracy of CCP for making a diagnosis of IP of 89%. This figure is significantly lower than the 97.8% reported by Maroldi et al.<sup>19</sup> The difference in the results between these 2 studies might be attributed to the difference in the inclusion of malignant tumors. A much greater number and wider variety of malignant tumors were included in our study (128 tumors; 14 histologic types) compared with theirs (23 tumors; 3 histologic types). The other possible explanation might be the difference in defining a CCP on MR images. Although it was not specifically mentioned in their study, we determined a CCP to be present not only in cases in which CCP was diffusely distributed but also in cases in which CCP was visible only in a portion. If the CCP had been defined to be present only when it was diffusely seen within the tumor in our study, this imaging pattern would have been more specific for benign IPs, because 4 of 8 IPs concomitant with SCC and 11 of 17 malignant sinonasal tumors showed a CCP visualized only partially.

The incidence of malignant change in an individual series of sinonasal IPs has been reported to range from 2% to 53%.<sup>3,7,9-11</sup> SCC is the most commonly associated malignant tumor. The carcinoma may actually arise within the IP or it may merely be associated with a histologically bland IP. Patients with IPs that are associated with carcinomas fall into 3 groups: group 1, those who have primarily an IP with only a small focus of carcinoma; group 2, those who have primarily a carcinoma with only a small focus of IP; and group 3, those who had a history of histologically documented IP and subsequently develop a carcinoma in the area in which the IP arose.<sup>3,10</sup> The first 2 groups are deemed synchronous, and group 3 is metachronous. Of all of the carcinomas associated with IPs, approximately 61% are synchronous and 39% are metachronous.<sup>10</sup> It would be very useful for determining the therapeutic plans if we could distinguish the IPs with associated SCC from those without it preoperatively, because more aggressive surgical approaches would be needed for the former. Although there has been a study demonstrating that a malignant tumor is associated with bilateral IP, hyperkeratosis, more than 2 mitotic figures per high-powered field, and presence of plasma cells,<sup>25</sup> most investigators believe that there are no discrete pathologic or clinical findings of IP associated with the future development of SCC.<sup>2</sup> In this context, we believe that, although the MR imaging features alone would not preclude biopsy of the sinonasal mass, they may help the surgeons with preoperative planning.

Our study shows that a focal loss of a CCP on MR imaging may be an additional sign that might indicate the presence of coexistent malignancy, seen in 4 (50%) of 8 IPs concomitant with SCC. Traditionally, malignancy is corroborated by aggressive bone destruction; multicentric soft tissue extension; and metastasis to submandibular, upper, midjugular, and retropharyngeal lymph nodes on radiologic examinations.<sup>14,26</sup> Although IP without associated carcinoma has been reported to cause bone destruction similar to malignant tumors,<sup>6,19,27</sup> extensive bone destruction should always raise the possibility of an associated carcinoma.<sup>10</sup> In our study, frank bone destruction with extrasinonasal extension, such as the orbit, in-

fratemporal fossa, and cranial cavity, was noted in 3 of 8 tumors with concomitant IP and SCC, making a diagnosis of associated malignancy easier. All of these 3 tumors were associated with focal loss of a CCP, which was most conspicuously noted at the area of bone destruction (Fig 2A). In one additional tumor with concomitant IP and SCC unaccompanied by bone destruction, a focal loss of a CCP was detected on MR images that might give a clue to the presence of malignancy at that area. Although exact MR-pathologic correlation could not be performed, because this is a retrospective study and also because most lesions were removed piecemeal, we believe that the areas of loss of CCP on MR imaging represent the approximate sites of malignancy on histology. Similarly, Maroldi et al<sup>19</sup> reported a case of concomitant IP and SCC, of which the MR images showed loss of CCP at the area of SCC proved pathologically. As reported by Ojiri et al,<sup>17</sup> however, a tumor with multiple small foci of SCC distributed throughout IP could demonstrate CCP diffusely throughout the lesion without a focal loss of it and, thus, could not be discriminated from the typical IP on MR images. We also experienced 4 similar cases in this study, in which it would be difficult to differentiate IPs concomitant with SCC from those without SCC (Fig 2B). Malignant sinonasal tumors with a diffuse CCP can also hardly be differentiated from IPs without coexistent SCC, as seen in 6 cases in our study (Fig 3A–C).

There are 2 serious limitations in this study. The first limitation is related to the statistical issue on the diagnostic performance. The proportion of IPs included in our series is approximately 19% (30 of 158), which is much greater than 0.5%–4.0% reported among the general population. The calculations of positive predictive value, negative predictive value, and accuracy are dependent on not only the proportion of the patients with the disease of interest but also the proportions of control patients with each different histology. Even the specificity depends on the proportions of different histologies among the control patients. Thus, the values calculated from this study may not reflect the values that would be encountered in clinical practice, if these proportions are not corrected. The second limitation is related to the retrospective nature of this study. For the histopathologic diagnosis of malignant sinonasal tumors, we simply relied on the pathologic diagnosis reported at the time of surgery. Because an exact 1:1 MR-pathologic correlation was not performed, the possibility of the presence of small foci of IP within the malignant tumor cannot entirely be excluded.

## Conclusion

A CCP is a reliable MR imaging feature of sinonasal IPs to differentiate them from various malignant sinonasal tumors with the overall accuracy of 89% in our study. However, even the presence of a diffuse CCP throughout the tumor on MR imaging does not always guarantee the diagnosis of benign IPs, because it also can be seen in IPs concomitant with SCC or

other malignant tumors. A focal loss of a CCP might be a clue to a preoperative prediction of IPs concomitant with malignancy.

## References

- Skolnik EM, Loewy A, Friedman JE. Inverted papilloma of the nasal cavity. *Arch Otolaryngol* 1966;84:61–67
- Melroy CT, Senior BA. Benign sinonasal neoplasms: a focus on inverting papilloma. *Otolaryngol Clin N Am* 2006;39:601–17
- Hyams VJ. Papillomas of the nasal cavity and paranasal sinuses. A clinicopathological study of 315 cases. *Ann Otol Rhinol Laryngol* 1971;80:192–206
- Suh KW, Facer GW, Devine KD, et al. Inverting papilloma of the nose and paranasal sinuses. *Laryngoscope* 1977;87:35–46
- Lawson W, Le Bengier J, Som P, et al. Inverted papilloma: an analysis of 87 cases. *Laryngoscope* 1989;99:1117–24
- Myers EN, Fernau JL, Johnson JT, et al. Management of inverted papilloma. *Laryngoscope* 1990;100:481–90
- Vrabec DP. The inverted Schneiderian papilloma. A 25-year study. *Laryngoscope* 1994;104:582–605
- Lawson W, Ho BT, Shaari CM, et al. Inverted papilloma: a report of 112 cases. *Laryngoscope* 1995;105:282–88
- Lesperance MM, Esclamado RM. Squamous cell carcinoma arising in inverted papilloma. *Laryngoscope* 1995;105:178–83
- Barnes L. Schneiderian papillomas and nonsalivary glandular neoplasms of the head and neck. *Mod Pathol* 2002;15:279–97
- Lawson W, Kaufman MR, Biller HF. Treatment outcomes in the management of inverted papilloma: an analysis of 160 cases. *Laryngoscope* 2003;113:1548–56
- Pasquini E, Sciarretta V, Farneti G, et al. Inverted papilloma: report of 89 cases. *Am J Otolaryngol* 2004;25:178–85
- Yousem DM, Fellows DW, Kennedy DW, et al. Inverted papilloma: evaluation with MR imaging. *Radiology* 1992;185:501–05
- Woodruff WW, Vrabec DP. Inverted papilloma of the nasal vault and paranasal sinuses: spectrum of CT findings. *AJR Am J Roentgenol* 1994;162:419–23
- Roobottom CA, Jewell FM, Kabala J. Primary and recurrent inverting papilloma: appearances with magnetic resonance imaging. *Clin Radiol* 1995;50:472–75
- Dammann F, Pereira P, Laniado M, et al. Inverted papilloma of the nasal cavity and the paranasal sinuses: using CT for primary diagnosis and follow-up. *AJR Am J Roentgenol* 1999;172:543–48
- Ojiri H, Ujita M, Tada S, et al. Potentially distinctive features of sinonasal inverted papilloma on MR imaging. *AJR Am J Roentgenol* 2000;175:465–68
- Oikawa K, Furuta Y, Oridate N, et al. Preoperative staging of sinonasal inverted papilloma by magnetic resonance imaging. *Laryngoscope* 2003;113:1983–87
- Maroldi R, Farina D, Palvarini L, et al. Magnetic resonance imaging findings of inverted papilloma: differential diagnosis with malignant sinonasal tumors. *Am J Rhinol* 2004;18:305–10
- Barnes L, Verbin RS, Gnepp DR. Diseases of the nose, paranasal sinuses, and nasopharynx. In: Barnes L, ed. *Surgical Pathology of the Head and Neck*. Vol 1. New York: Marcel Dekker; 1985:403–51
- Shanmugaratnam K, Sobin LH. The World Health Organization histological classification of tumours of the upper respiratory tract and ear. A commentary on the second edition. *Cancer* 1993;71:2689–97
- Lai PH, Yang CF, Pan HB, et al. Recurrent inverted papilloma: diagnosis with pharmacokinetic dynamic gadolinium-enhanced MR imaging. *AJNR Am J Neuroradiol* 1999;20:1445–51
- Petit P, Vivarrat-errin L, Champsaur P, et al. Radiological follow-up of inverted papilloma. *Eur Radiol* 2000;10:1184–89
- Lee DK, Chung SK, Dhong HJ, et al. Focal hyperostosis on CT of sinonasal inverted papilloma as a predictor of tumor origin. *AJNR Am J Neuroradiol* 2007;28:618–21
- Wormald PJ, Ooi E, van Hasselt CA, et al. Endoscopic removal of sinonasal inverted papilloma including endoscopic medial maxillectomy. *Laryngoscope* 2003;113:867–73
- Som PM, Brandwein MS. Lymph nodes. In: Som PM, Curtin HD, eds. *Head and Neck Imaging*, 4th ed. St Louis: Mosby; 2003:1881
- Som PM, Lawson W, Lidov MW. Simulated aggressive skull base erosion in response to benign sinonasal disease. *Radiology* 1991;180:755–59